



## Priority Communication

Surface science approach to catalyst preparation – Pd deposition onto thin  $\text{Fe}_3\text{O}_4(111)$  films from  $\text{PdCl}_2$  precursorHui-Feng Wang, Hiroko Ariga<sup>1</sup>, Rhys Dowler, Martin Sterrer\*, Hans-Joachim Freund*Department of Chemical Physics, Fritz-Haber-Institut der Max-Planck-Gesellschaft, Faradayweg 4-6, 14195 Berlin, Germany*

## ARTICLE INFO

*Article history:*

Received 23 August 2011  
 Revised 21 September 2011  
 Accepted 22 September 2011  
 Available online 22 October 2011

*Keywords:*

Catalyst preparation  
 Surface science approach  
 Thin film  
 Impregnation  
 Palladium  
 Iron oxide  
 Scanning tunneling microscopy  
 X-ray photoelectron spectroscopy

## ABSTRACT

In this work, we introduce a surface science approach to supported metal catalyst preparation utilizing thin, single-crystalline oxide films as substrates. The use of thin oxide films allows for combined morphological and chemical characterization of the sample at various steps of a typical catalyst preparation procedure. A  $\text{Fe}_3\text{O}_4$ -supported Pd model catalyst was prepared by impregnation of  $\text{Fe}_3\text{O}_4(111)$  films with acidic  $\text{PdCl}_2$  solution, and the transformation of the adsorbed precursor into supported Pd nanoparticles by stepwise heating in vacuum was followed with scanning tunneling microscopy (STM) and X-ray photoelectron spectroscopy (XPS). The results provide evidence for homogeneous nucleation of Pd particles out of a monolayer of adsorbed precursor and an enhancement of the particle-support interaction with increasing annealing temperature. Chlorine, which remains on the model catalyst surface after vacuum annealing, could be removed by oxidation/reduction. This treatment also leads to particle sintering with an increase in the average particle diameter from 2 nm to 4 nm after oxidation/reduction.

© 2011 Elsevier Inc. All rights reserved.

## 1. Introduction

The preparation of supported metal catalysts is a complex multi-step procedure [1,2]. In the most commonly applied preparation route, impregnation, the first step involves the interaction of aqueous solutions containing metal precursors with the support, followed by drying, calcination, and reduction to transform the metal precursor into the catalytically active compound. Clearly, catalytic activity in a given test reaction is the ultimate criterion for the usefulness of a specific preparation procedure and is often combined with pre, in situ or post-reaction characterization to determine the physical (particle size and shape) and chemical (oxidation state, chemisorption) properties of the active catalyst and to reveal details about the reaction mechanism. Maximizing the abundance and stability of active sites requires, in turn, molecular level control and an understanding of the important steps during catalyst preparation and activation [3–7].

Surface science experiments using morphologically well-defined samples contributed to a great extent to the atomic level understanding of catalytically active metals. It is highly desirable to extend such studies and therefore the benefit of ultimate mor-

phological control to the important field of supported metal catalyst preparation. Previous attempts related to metal deposition from liquid phase precursors onto flat oxide substrates (single crystal surfaces and single crystal fragments, or noncrystalline oxide thin films) provided some relevant insights; however, they lack of combined morphological and chemical characterization [8–13]. In the approach presented herein, we take advantage of the ability to reproducibly grow under ultra-high vacuum (UHV) conditions thin, single-crystalline oxide films with well-defined morphology, which allow typical surface science analysis tools to be applied and use them as substrates for studying the formation of supported metal nanoparticles following wet chemical catalyst preparation procedures.

As a prototype system, we have chosen to use  $\text{Fe}_3\text{O}_4(111)$  films grown on Pt(111) as substrate for Pd nanoparticles. UHV-deposited Pd nanoparticles on  $\text{Fe}_3\text{O}_4$  have been extensively investigated in our laboratory in the past and served as a model system for detailed studies of Pd nanoparticle reactivity in oxidation and hydrogenation reactions [14,15]. The UHV preparation route is exceptionally clean and does not include possible chemical interference from the precursor used in realistic preparations. In particular, catalysts prepared via impregnation with  $\text{PdCl}_2$ , the most frequently used precursor for supported Pd catalysts [16], retain chlorine, which has been shown to act as a poison in certain catalytic applications, supposedly by blocking the active sites [17–19]. Here, we report on the preparation of a  $\text{Fe}_3\text{O}_4(111)$ -supported Pd

\* Corresponding author.

E-mail address: [sterrer@fhi-berlin.mpg.de](mailto:sterrer@fhi-berlin.mpg.de) (M. Sterrer).<sup>1</sup> Present address: Catalysis Research Center, Hokkaido University, Kita-ku, North 21 West 10, Sapporo 001-0021, Japan.

model catalyst from acidic  $\text{PdCl}_2$  precursor solution. The combined use of scanning tunneling microscopy (STM) and X-ray photoelectron spectroscopy (XPS) allows both the morphological and chemical changes that come along with the transformation of the adsorbed Pd precursor into nanoparticles in the early stages of catalyst preparation to be tracked.

## 2. Methods

The experimental set up consists of a UHV chamber equipped with a sputter gun, a metal evaporator, a low energy electron diffraction (LEED) apparatus, and an XPS system for single crystal cleaning, preparation, and characterization. The  $\text{Fe}_3\text{O}_4(111)$  films were grown on a Pt(111) substrate as described in detail previously [20]. Briefly, one monolayer of Fe was evaporated onto clean Pt(111) at room temperature (RT) and subsequently oxidized at 1000 K for 2 min to form a  $\text{FeO}(111)$  monolayer film. This served as substrate for a  $\sim 10$  nm thick  $\text{Fe}_3\text{O}_4(111)$  film, which was grown by repeated cycles of  $\sim 8$  ML Fe deposition at RT and oxidation at  $\sim 900$  K. Finally, the film was oxidized at  $\sim 1000$  K in  $10^{-6}$  mbar  $\text{O}_2$  for 10 min.

The Pd precursor stock solution was prepared by dissolving  $\text{PdCl}_2$  (99.9%, Alfa Aesar) in 5 M HCl. This stock solution was diluted with  $\text{H}_2\text{O}$  to yield a final Pd concentration of 15 mM and pH 1.3. For impregnation with precursor solution as well as STM experiments, the sample was transferred via a load lock out of the UHV chamber. The supported Pd catalyst was prepared by the following procedure: Firstly, the  $\text{Fe}_3\text{O}_4(111)$  surface was contacted with acidic  $\text{PdCl}_2$  solution (pH 1.3, 15 mM) for 1 h at RT. Then, the solution was removed and the surface rinsed four times with ultra-pure water at RT. Rinsing with water was necessary to remove residual precursor solution from the single crystal surface, which could lead to unwanted precipitation of  $\text{PdCl}_2$  in the subsequent drying step. Drying was carried out at RT under a stream of He gas. Subsequent heating to elevated temperatures (390 and 600 K) as well as oxidation ( $\text{O}_2$ ) and reduction (CO) treatments were performed in the UHV chamber. A gas atmosphere of  $1 \times 10^{-6}$  mbar during oxidation (reduction) was sufficient to induce the desired chemical changes of the supported Pd particles and low enough to avoid transformation of  $\text{Fe}_3\text{O}_4$  into  $\text{Fe}_2\text{O}_3$ , which could occur at elevated temperature under more realistic oxygen partial pressures in the mbar range [20].

STM measurements were conducted in air using a Wandelt-type STM [21] directly after drying as well as after additional thermal pretreatment and oxidation/reduction steps. All STM images reported in this work were acquired at a tunneling current of

$i_t = 0.1$  nA and a bias voltage of  $U_t = -0.3$  V. XPS spectra were acquired in UHV using an Al  $K\alpha$  X-ray source and a hemispherical analyzer (SPECS Phoibos 150).

## 3. Results and discussion

In Fig. 1a, we present an STM image of the surface of a  $\sim 10$  nm thick  $\text{Fe}_3\text{O}_4(111)$  film taken in air. Similar to previous UHV studies, we observe large terraces separated by well-defined step edges [22]. As shown in Fig. 1b, the surface morphology remains essentially unchanged after exposing the sample to HCl (pH 1.3) solution for 60 min. The fact that the  $\text{Fe}_3\text{O}_4$  surface is resistant to attack from the acidic solution makes it an ideal starting material for the following investigation of Pd deposition from acidic Pd precursor solution.

For impregnation, the  $\text{Fe}_3\text{O}_4(111)$  surface was exposed at room temperature for 60 min to 15 mM  $\text{PdCl}_2$  (pH 1.3) solution. The STM image obtained after removing the solution, rinsing the sample with water, and subsequent drying with He at RT shows a low density of particles on otherwise seemingly “clean”  $\text{Fe}_3\text{O}_4(111)$  terraces (Fig. 2a, left). Comparison of Fig. 2a (left) with the STM image of the  $\text{Fe}_3\text{O}_4(111)$  surface exposed to HCl solution shown in Fig. 1b, where only flat terraces without any adsorbate are imaged, allows to attribute the particles observed at this stage to Pd species and not to impurities such as carbon that accumulates on the surface during air exposure. In addition, atomic resolution imaging that can be frequently achieved on terraces of the clean  $\text{Fe}_3\text{O}_4(111)$  surface even in ambient air was not possible on a surface exposed to precursor solution. This indicates chemical changes of the surface induced by exposure to the precursor solution, which can intuitively be related to the presence of adsorbed molecular precursor. In a next step, the sample was dried at 390 K in UHV, whereupon the particle density increases (Fig. 2a, middle). Finally, after heating to 600 K in UHV, particles cover the entire oxide surface (Fig. 2a, right). The sequence of STM images in Fig. 2a indicates reduction of the adsorbed molecular Pd precursor, which cannot be resolved in our STM experiment, to Pd particles by heating in UHV. XPS results presented below support this conclusion. Meanwhile, additional information regarding the nucleation behavior and the particle-support interaction can be deduced: STM images obtained directly after impregnation as well as after drying at 390 K show randomly distributed particles on the oxide surface, while they uniformly cover the surface after heating to 600 K (Fig. 2a). Note that there is no preferential nucleation at surface irregularities such as step edges. This observation provides strong evidence for homogeneous nucleation

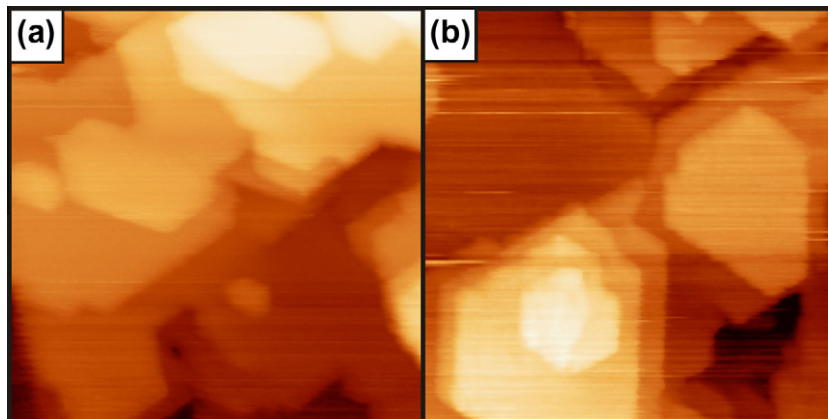
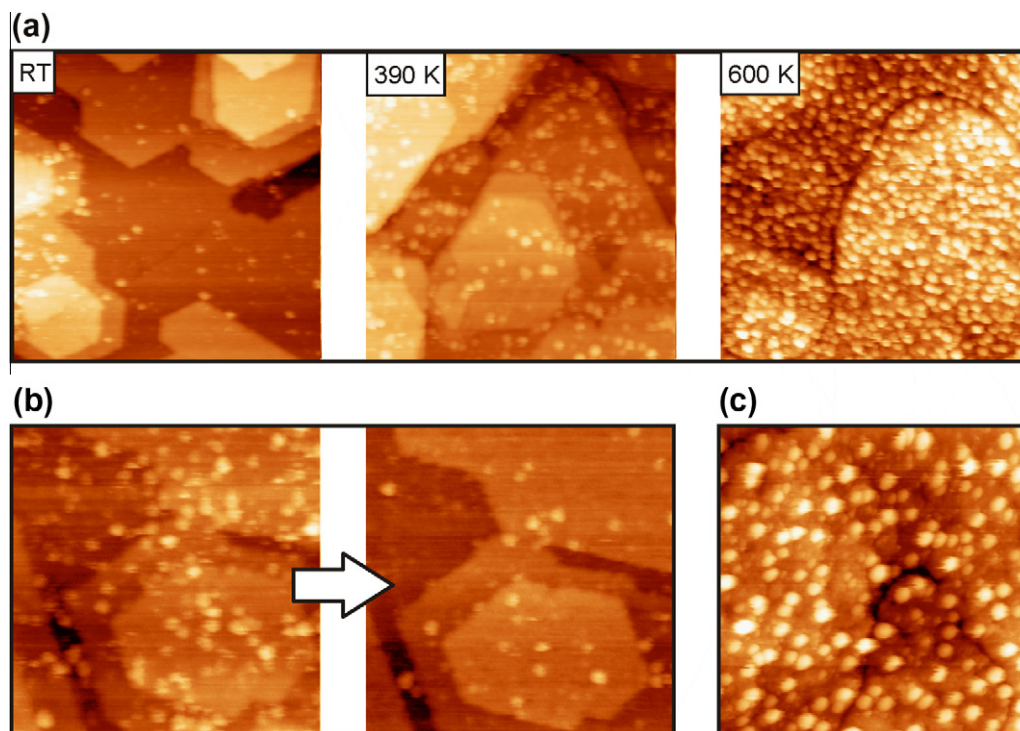


Fig. 1. STM images ( $100 \text{ nm} \times 100 \text{ nm}$ ) of  $\text{Fe}_3\text{O}_4(111)/\text{Pt}(111)$  taken in air directly after preparation (a), and after exposure to HCl (pH 1.3, 60 min) and subsequent drying (b).



**Fig. 2.** (a) Series of STM images ( $100 \text{ nm} \times 100 \text{ nm}$ ) of  $\text{Fe}_3\text{O}_4(111)/\text{Pt}(111)$  taken in air after contact with  $\text{PdCl}_2$  (pH 1.3) solution (left) directly after removing the solution, (middle) after UHV-annealing at 390 K, and (right) after UHV-annealing at 600 K. (b) STM images ( $70 \text{ nm} \times 70 \text{ nm}$ ) showing the same area of  $\text{Fe}_3\text{O}_4(111)/\text{Pt}(111)$  exposed to  $\text{PdCl}_2$  (pH 1.3) and annealed to 390 K in subsequent STM scans. The majority of particles present in the left image is only weakly bound to the surface and easily removed by the STM tip. (c) STM image ( $100 \text{ nm} \times 100 \text{ nm}$ ) of the  $\text{Fe}_3\text{O}_4(111)$  and  $\text{PdCl}_2$  (pH 1.3) sample after 600 K annealing and additional oxidation and reduction treatment to remove chlorine.

of Pd particles from a monolayer of adsorbed precursor. The diameter of the particles observed in Fig. 2a is  $\sim 2 \text{ nm}$  regardless of the pretreatment temperature used in this study showing that 600 K is well below the onset of Ostwald ripening. We observed, however, a strong dependence of the particle-support interaction on the pretreatment temperature. The particles on the dried sample (RT, 390 K) could easily be moved under the STM tip by increasing the bias voltage. This is exemplified in Fig. 2b, which presents images of the same area of a sample dried at 390 K scanned successively. The majority of small particles present in the left image of Fig. 2b disappeared after additional scanning (compare with right image of Fig. 2b) either by moving with or collection by the STM tip (increasing the scan area after scanning at high bias revealed that some particles accumulated at the edges of the previous scan window). This suggests that the particles are only weakly bound to the support at this stage of preparation. In contrast, no such behavior was observed for the sample heated to 600 K indicating a clear enhancement of the particle-support interaction by heating.

The chemical nature of the surface species present at the various stages of sample pretreatment was studied with XPS (Fig. 3). The spectra obtained directly after removing the solution contain a dominant Pd  $3d_{5/2}$  component at a binding energy (BE) of 337.8 eV, and a second Pd  $3d_{5/2}$  component at 336.2 eV. With increasing temperature, a gradual transformation of the high BE component into the low BE component and a shift to lower BE is evident (Fig. 3a). Comparison with the STM images in Fig. 2a allows the emergence of the low BE peak with the abundance of nucleated particles, which increases with pretreatment temperature, to be directly correlated. Similarly, the loss of the high BE peak reflects the thermal decomposition of the Pd precursor complex. Analysis of the Fe 2p (not shown) and Pd 3d XPS peak intensities shows a clear increase in the Fe/Pd ratio with increasing annealing temperature. This expected trend can be rationalized in terms of weaker atten-

uation of the Fe 2p emission once Pd particles have been formed after high temperature treatment. This leads to a higher fraction of  $\text{Fe}_3\text{O}_4$  surface exposed to vacuum as compared to the state directly after precursor deposition, where the  $\text{Fe}_3\text{O}_4$  surface is homogeneously covered by Pd precursor complexes.

Apart from this qualitative correlation, the measured BE's may further be analyzed to determine the chemical identity of the surface species. For the species relevant in this study, the Pd  $3d_{5/2}$  BE increases in the order as follows:  $\text{Pd}^0$  (335.2 eV) <  $\text{Pd}^{\delta+}\text{Cl}^-$  <  $\text{Pd}(\text{H}_2\text{O})_x \text{Cl}_y^{n+(-)}$  (336–338 eV)  $\leq$   $\text{PdCl}_2$  (337.8 eV) <  $\text{PdCl}_4^{2-}$  (338.1 eV) [23,24]. It is well documented that during impregnation with acidic  $\text{PdCl}_2$  solution predominantly  $\text{PdCl}_4^{2-}$  ions adsorb on the support surface. The high BE component at 337.8 eV observed after impregnation, washing, and drying at RT is well below the Pd  $3d_{5/2}$  BE in  $\text{PdCl}_4^{2-}$  and is instead assigned to adsorbed aquochloro complexes,  $\text{Pd}(\text{H}_2\text{O})_x \text{Cl}_y^{n+(-)}$ . In fact, a rough estimate of the elemental distribution from the Pd 3d (Fig. 3a) and Cl 2p (Fig. 3b) peak areas gives a Pd/Cl atomic ratio of  $\sim 1:1$ , clearly different than expected for  $\text{PdCl}_4^{2-}$ . The change of the nature of the adsorbed precursor may be explained by respeciation of  $\text{PdCl}_4^{2-}$  upon adsorption because of the increase in the local pH above the support surface. Such phenomenon has been observed for the interaction of  $\text{PdCl}_4^{2-}$  with alumina support when precursor solutions with  $\text{pH} > 3$  were used [25]. Since the pH of the precursor solution (pH 1.3) used in the present experiment is well below this threshold pH (and similar behavior of alumina and iron oxide supports may be expected because of the similar point of zero charge,  $\text{pzc} \approx 8$ , of the two oxides), we exclude the possibility of respeciation because of variation of the local pH and rather attribute the change of the nature of the adsorbed precursor to ligand exchange during the washing step. Ligand exchange results in particular in the formation of neutral or singly charged aquochloro complexes for which the lateral repulsive interaction on the surface is signif-

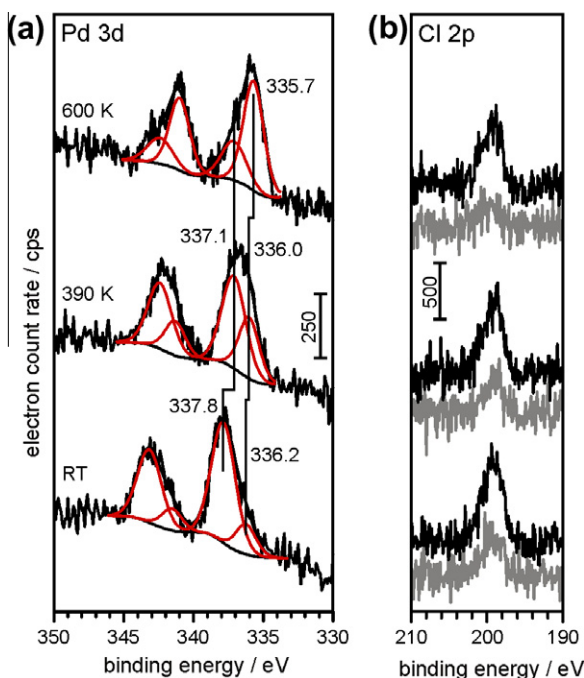


**Fig. 3.** (a) Pd 3d ( $E_{\text{pass}} = 20$  eV), and (b) Cl 2p ( $E_{\text{pass}} = 50$  eV) photoemission spectra of  $\text{Fe}_3\text{O}_4(111)$  exposed to  $\text{PdCl}_2$  (pH 1.3). The spectra were recorded (bottom) directly after exposure to  $\text{PdCl}_2$  solution at RT, (middle) after subsequent annealing to 390 K, and (top) after further annealing to 600 K. The Cl 2p spectra of a  $\text{Fe}_3\text{O}_4(111)$  sample that has been exposed to HCl (pH 1.3, blank experiment) are shown as gray traces in (b).

icantly reduced as compared to adsorbed  $\text{PdCl}_4^{2-}$ . Hence, the possibility to form agglomerates is enhanced and this may account for the observation of the small number of Pd particles on the sample dried at room temperature after the washing step (Fig. 2a, left). Upon heating the sample to 390 and 600 K, the high BE component shifts from 337.8 to 337.1 eV, which is most probably related to partial decomposition of the adsorbed precursor complexes.

The second Pd  $3d_{5/2}$  signal related to the nucleated particles exhibits a BE of 336.2 eV (RT), which shifts to 335.7 eV upon heating to 600 K (Fig. 3a). These values are higher than expected for metallic Pd particles, but considerably lower than expected for  $\text{PdCl}_2$ . Two effects may contribute in the present study to the observed positive BE shift with respect to bulk Pd: (i) particle size-dependent screening of the Pd core hole created in the photoemission process, resulting in higher BE's for small particles as compared to bulk Pd [26–29]. (ii) Formation of  $\text{Pd}^{\delta+}$  species by charge transfer to Cl which remains adsorbed on the surface of the particles. While a rigorous separation of the two contributions is not possible, the Cl 2p XP spectra reported in Fig. 3b provide strong evidence for remaining Cl on the Pd particles. We find that, whereas the chlorine-containing precursor is gradually transformed into Pd nanoparticles, the surface chlorine concentration is not affected by thermal treatment (Fig. 3b, black traces). Furthermore, in a blank experiment with the  $\text{Fe}_3\text{O}_4$  surface exposed to HCl (pH 1.3) solution without Pd precursor, the amount of chlorine is considerably less and it could almost completely be removed by heating to 600 K (gray traces in Fig. 3b). The chlorine detected after heating the Pd-containing sample to 600 K can, therefore, unambiguously be related to the Pd particles. This result is in line with the high desorption temperature ( $\sim 1000$  K) that has been reported for chlorine on Pd surfaces [30].

Since chlorine is an unwanted residue of the preparation process, the sample was further subjected to oxidation ( $1 \times 10^{-6}$  mbar  $\text{O}_2$ , 600 K, 5 h) and subsequent reduction ( $1 \times 10^{-6}$  mbar CO, 500 K, 1 h) [31]. No chlorine could be detected with XPS afterward.

However, the oxidation/reduction treatment resulted in morphological changes as seen in STM: The average Pd particle diameter increased from 2 nm before (Fig. 2b, right), to 4 nm after oxidation/reduction (Fig. 2c). Particle sintering (and chlorine removal) occurred mainly during oxygen treatment, in accord with a recent UHV study that showed that the formation of surface and interface oxides is responsible for Pd sintering on  $\text{Fe}_3\text{O}_4$  under mild oxidation conditions [32]. The facile removal of chlorine observed here is related to the rather weak interaction of the  $\text{Fe}_3\text{O}_4(111)$  surface with HCl, as demonstrated by the XPS results in Fig. 3b. In this respect, the  $\text{Fe}_3\text{O}_4(111)$  support is similar to silica supports, where chlorine can easily be removed by reduction (in contrast to alumina) [23]. In addition, and as already stated previously, the absence of diffusion limitation and readsorption on a flat substrate as opposed to porous support materials might influence the retention of chlorine [9].

#### 4. Conclusion

We presented a new approach that allows, by utilizing thin, single-crystalline oxide films as substrates, both morphological and chemical information during the early stages of supported metal catalyst preparation to be gained. We have in particular investigated the thermal transformation of Pd precursor complexes into metal nanoparticles on  $\text{Fe}_3\text{O}_4(111)$ . STM experiments revealed that during heating Pd particles homogeneously nucleate from the adsorbed molecular precursor after impregnation of  $\text{Fe}_3\text{O}_4(111)$  with acidic  $\text{PdCl}_2$  solution and that the particle-support interaction is temperature dependent. In addition, the morphological information is important for the interpretation of the spectroscopic data and helps in the assignment of the XPS signals. Residual chlorine is found to be mainly in contact with the Pd particles and could be easily removed by oxidation/reduction, which also leads to particle sintering.

The approach presented herein offers great potential for further elucidation of catalyst preparation procedures. In particular, variation of parameters such as pH of the impregnation solution as well as concentration and type of precursor salt and, hence, the different nucleation behavior and chemical identity of surface species may contribute to a better understanding of the influence of preparation parameters on the final properties of a catalyst. We envisage to further extend this approach to in situ microscopic and spectroscopic studies of the oxide-solution interface during the impregnation step, which could reveal in detail the adsorption behavior of precursor complexes.

#### Acknowledgments

H.-F.W. thanks the International Max Planck Research School “Complex Surfaces in Materials Science” for a fellowship. This work was supported by the Cluster of Excellence “Unifying Concepts in Catalysis” sponsored by Deutsche Forschungsgemeinschaft (DFG) and administered by TU Berlin.

#### References

- [1] G. Ertl, H. Knözinger, F. Schüth, J. Weitkamp (Eds.), Handbook of Heterogeneous Catalysis, Wiley-VCH, Weinheim, 2008.
- [2] K.P. de Jong (Ed.), Synthesis of Solid Catalysts, Wiley-VCH, Weinheim, 2009.
- [3] J.-F. Lambert, M. Che, J. Mol. Catal. A 162 (2000) 5.
- [4] M. Schreier, J.R. Regalbutto, J. Catal. 225 (2004) 190.
- [5] J.A. Bergwerff, A.A. Lysova, L. Espinosa Alonso, I.V. Koptuyug, B.M. Weckhuysen, Angew. Chem. Int. Ed. 46 (2007) 7224.
- [6] P.J. Chupas, K.W. Chapman, G. Jennings, P.L. Lee, C.P. Grey, J. Am. Chem. Soc. 129 (2007) 13822.
- [7] G. Agostini, E. Groppo, A. Piovano, R. Pellegrini, G. Leofanti, C. Lamberti, Langmuir 26 (2010) 11204.
- [8] L.M. Eshelman, A.M. de Jong, J.W. Niemantsverdriet, Catal. Lett. 10 (1991) 201.

- [9] H.J. Borg, L.C.A. van den Oetelaar, J.W. Niemantsverdriet, *Catal. Lett.* 17 (1993) 81.
- [10] C. Doornkamp, C. Laszla, W. Wieldraaijer, E.W. Kuipers, *J. Mater. Res.* 10 (1995) 411.
- [11] D.P.C. Bird, C.M.C. de Castilho, R.M. Lambert, *Surf. Sci.* 449 (2000) L221.
- [12] T. Akita, M. Okumura, K. Tanaka, M. Haruta, *J. Catal.* 212 (2002) 119.
- [13] C. Park, P.A. Fenter, N.C. Sturchio, J.R. Regalbuto, *Phys. Rev. Lett.* 94 (2005) 076104.
- [14] T. Schalow, M. Laurin, B. Brandt, S. Schauerermann, S. Guimond, H. Kühlenbeck, D.E. Starr, S. Shaikhutdinov, J. Libuda, H.-J. Freund, *Angew. Chem. Int. Ed.* 44 (2005) 7601.
- [15] M. Wilde, K. Fukutani, W. Ludwig, B. Brandt, J.-H. Fischer, S. Schauerermann, H.-J. Freund, *Angew. Chem. Int. Ed.* 47 (2008) 9289.
- [16] M.L. Toebes, J.A. van Dillen, K.P. de Jong, *J. Mol. Catal. A* 173 (2001) 75.
- [17] D.O. Simone, T. Kennelly, N.L. Brungard, R.J. Farrauto, *Appl. Catal.* 70 (1991) 87.
- [18] N. Mahata, V. Vishwanathan, *J. Catal.* 196 (2000) 262.
- [19] T. Lear, R. Marshall, J.A. Lopez-Sanchez, S.D. Jackson, T.M. Klapötke, M. Bäumer, G. Rupprechter, H.-J. Freund, D. Lennon, *J. Chem. Phys.* 123 (2005) 174706.
- [20] W. Weiss, M. Ritter, *Phys. Rev. B* 59 (1999) 5201.
- [21] M. Wilms, M. Kruft, G. Bermes, K. Wandelt, *Rev. Sci. Instrum.* 70 (1999) 3641.
- [22] Sh.K. Shaikhutdinov, M. Ritter, X.-G. Wang, H. Over, W. Weiss, *Phys. Rev. B* 60 (1999) 11062.
- [23] F. Bozon-Verduraz, A. Omar, J. Escard, B. Pontvianne, *J. Catal.* 53 (1978) 126.
- [24] T.H. Fleisch, R.F. Hicks, A.T. Bell, *J. Catal.* 87 (1984) 398.
- [25] J.R. Regalbuto, in: K.P. de Jong (Ed.), *Synthesis of Solid Catalysts*, Wiley-VCH, Weinheim, 2009, p. 45.
- [26] W.F. Egelhoff, G.G. Tibbetts, *Phys. Rev. B* 19 (1979) 5028.
- [27] M.G. Mason, *Phys. Rev. B* 27 (1983) 748.
- [28] G.K. Wertheim, S.B. DiCenzo, S.E. Youngquist, *Phys. Rev. Lett.* 51 (1983) 2310.
- [29] F.A. Marks, I. Lindau, R. Browning, *J. Vac. Sci. Technol. A* 8 (1990) 3437.
- [30] W.T. Tysoe, R.M. Lambert, *Surf. Sci.* 199 (1988) 1.
- [31] We used CO instead of H<sub>2</sub> as reducing agent because reduction in H<sub>2</sub> atmosphere leads to strong chemical modification of both the Pd particles and the Fe<sub>3</sub>O<sub>4</sub> substrate.
- [32] T. Schalow, B. Brandt, D.E. Starr, M. Laurin, S. Schauerermann, S. Shaikhutdinov, J. Libuda, H.-J. Freund, *Catal. Lett.* 107 (2006) 189.